

Classification of Rotated and Scaled Textured Images Using Spectral Moments

Yasuo YOSHIDA *

Department of Electronics
and Information Science,
Kyoto Institute of Technology

Yue WU †

Central R&D Laboratory,
Omron Corporation

Abstract

This paper describes a classification method for rotated and scaled textured images using invariant parameters based on spectral-moments. Although it is well known that rotation invariants can be derived from moments of grey-level images, the use is limited to binary images because of its computational unstability. In order to obtain computationally stable moments, we use power spectrum instead of the grey levels to compute moments and adjust an integral region to scale change. Rotation and scale invariants are obtained as the ratio of the rotation invariants on the basis of a spectral-moment property with respect to scale. The effectiveness of the approach is illustrated through experiments on natural textures from the Brodatz album. The stability of the invariants with respect to change of scale is discussed theoretically and confirmed experimentally.

1 Introduction

A variety of texture classification approaches has been studied over the past decades. Most of these approaches address the classification problem under the assumption that a test textured image possesses the same orientation and scale as training images. They perform poorly even though the orientation or the scale of the test image differs a little from those of the training ones. However, there are a few papers dealing with classification of both rotated and scaled images. Cohen et al. have proposed such method [1] that the spectral density function (SDF) of a standard image is rotated and scaled so as to match it to that of a test image. It performs excellent but it seems computationally unattractive. We have proposed the method [2] that rotation and scale (RS) invariants are obtained from spectral peak locations and from model parameters of the SDF fitted to an image. The technique is fast but its performance is not very satisfactory.

This paper proposes a fast and efficient technique based on RS invariants obtained from spectral moments. Rotation invariants derived from moments have been studied by many researchers. However, successful results for pattern recognition using them are limited only to binary images with a finite-sized object[3][4]. Application of the moments to grey-scale images is difficult because the images have non-zero values on the image boundaries, which makes the moment invariants computationally unstable if they are rotated or scaled. Instead of the grey-level moments of the image, we use the moments of its SDF to obtain rotation invariants because the SDF has advantageous properties. When an image is rotated and scaled, its SDF rotates by the same angle and is inversely scaled; moreover, the spectral powers of most textured images are compact around the origin. In addition, we scheme to obtain stable rotation moments; we define as a circle the integral region for moment calculation and adjust its radius to scale change by setting a constant rate of the image total power in the circle. Since spectral moments have a simple property with respect to scale, we can obtain RS invariants defined as a ratio of rotation invariants. Next, we confirm the validity of the proposed method in experiments using textures from Brodatz album. Last, we examine the stabilities of the rotation invariants and the RS invariants theoretically and experimentally and conclude that the RS invariants have excellent robustness.

2 Spectral Moments

We assume that the discrete image $f(m, n)$ has been normalized to have zero mean and unit variance. So that the technique introduced below should not be affected by a linear change in the illumination of the image. The SDF of $f(m, n)$ is denoted by $S(\omega, \nu)$, $(-\pi \leq \omega, \nu \leq \pi)$. Moreover, we assume that the sampling period is such that no aliasing occurs in the SDF $S(\omega, \nu)$. When the test image $f(m, n)$ is rotated by an angle θ and scaled by a factor α , i.e.,

$$\begin{aligned} f_T(m, n) &= f\{(m \cos \theta + n \sin \theta)/\alpha, \\ &\quad (-m \sin \theta + n \cos \theta)/\alpha\}, \end{aligned} \quad (1)$$

* Address: Matsugasaki, Sakyo-ku, Kyoto-shi 606, Japan,
E-mail: yyoshida@dj.kit.ac.jp

† Address: Shimokaijinji, Nagaokakyo-shi, Kyoto 617,
Japan, E-mail: wu@rbc.ncl.omron.co.jp

its SDF rotates by the same angle and is inversely scaled[1], which is given by,

$$\begin{aligned} S_T(\omega, \nu) &= \alpha^2 S\{(\alpha(\omega \cos \theta + \nu \sin \theta), \\ &\quad \alpha(-\omega \sin \theta + \nu \cos \theta))\}. \end{aligned} \quad (2)$$

We define the $(p+q)$ th order spectral moment as

$$\begin{aligned} \mu_{p,q}(\alpha, \theta) &= \iint_{\sqrt{\omega^2+\nu^2} \leq R(\alpha)} \omega^p \nu^q S_T(\omega, \nu) d\omega d\nu. \end{aligned} \quad (3)$$

In order to obtain RS invariants, it is necessary to use the same part of the SDF for computing moments even when the image is rotated and scaled. Therefore, the integral region is assumed to be a circle with the radius $R(\alpha)$, which is inversely proportional to the scale factor α . Because α is unknown, we determine the $R(\alpha)$ by

$$\begin{aligned} &\iint_{\sqrt{\omega^2+\nu^2} \leq R(\alpha)} S_T(\omega, \nu) d\omega d\nu \\ &= \gamma \int_{-\pi}^{\pi} \int_{-\pi}^{\pi} S_T(\omega, \nu) d\omega d\nu \end{aligned} \quad (4)$$

where γ is a constant and $0 < \gamma < 1$. The left hand side of (4) is the 0th order spectral moment, and the right hand side represents a part(γ) of the total image power. From (2) and (3), we obtain the spectral moment property with respect to scale

$$\mu_{p,q}(\alpha, \theta) = \frac{\mu_{p,q}(1, \theta)}{\alpha^{p+q}}. \quad (5)$$

Because the SDF of an image is symmetrical, i.e., $S(\omega, \nu) = S(-\omega, -\nu)$, the odd-order spectral moments are always zero. We search for rotation invariants represented in terms of the usual moments.

In order to construct the rotation invariants, we introduce rotational moments [5] defined by,

$$\begin{aligned} D_{n,l} &= \iint_{\sqrt{\omega^2+\nu^2} \leq R(\alpha)} r^n e^{-il\theta} S_T(\omega, \nu) d\omega d\nu, \\ n &= 0, 2, 4, \dots, l &= 0, 2, \dots, n \end{aligned} \quad (6)$$

$$r = \sqrt{\omega^2 + \nu^2}. \quad (7)$$

From the symmetric property of the SDF, $D_{n,l}$ vanishes if n or l is an odd integer. Using $D_{n,l}$ and its relation to the usual moments, we obtain the following rotation invariants:

Second order

$$I_{2,0} = D_{2,0} = \mu_{2,0} + \mu_{0,2} \quad (8)$$

$$I_{2,1} = |D_{2,2}|^2 = (\mu_{2,0} - \mu_{0,2})^2 + 4\mu_{1,1}^2 \quad (9)$$

Fourth order

$$I_{4,0} = D_{4,0} = \mu_{4,0} + 2\mu_{2,2} + \mu_{0,4} \quad (10)$$

$$I_{4,1} = |D_{4,2}|^2$$

$$= (\mu_{4,0} - \mu_{0,4})^2 + 4(\mu_{3,1} + \mu_{1,3})^2 \quad (11)$$

$$\begin{aligned} I_{4,2} &= |D_{4,4}|^2 \\ &= (\mu_{4,0} - 6\mu_{2,2} + \mu_{0,4})^2 \\ &\quad + 16(\mu_{3,1} - \mu_{1,3})^2 \end{aligned} \quad (12)$$

$$\begin{aligned} I_{4,3} &= \text{Re}(D_{4,2} \overline{D_{2,2}}) \\ &= (\mu_{4,0} - \mu_{0,4})(\mu_{2,0} - \mu_{0,2}) \\ &\quad + 4\mu_{1,1}(\mu_{3,1} + \mu_{1,3}) \end{aligned} \quad (13)$$

$$\begin{aligned} I_{4,4} &= \text{Re}(D_{4,4} \overline{D_{2,2}}) \\ &= (\mu_{4,0} - 6\mu_{2,2} + \mu_{0,4}) \\ &\quad \times \{(\mu_{2,0} - \mu_{0,2})^2 - 4\mu_{1,1}^2\} \\ &\quad + 16\mu_{1,1}(\mu_{3,1} - \mu_{1,3})(\mu_{2,0} - \mu_{0,2}) \end{aligned} \quad (14)$$

Sixth order

$$I_{6,0} = D_{6,0} = \mu_{6,0} + 3\mu_{4,2} + 3\mu_{2,4} + \mu_{0,6} \quad (15)$$

Eighth order

$$I_{8,0} = D_{8,0} = \mu_{8,0} + 4\mu_{6,2} + 6\mu_{4,4} + 4\mu_{2,6} + \mu_{0,8} \quad (16)$$

For simplicity, with regard to the sixth and eighth order moments, we only take the radial-moment invariants that is independent of angular distribution of the SDF.

The defined features $\{I_{n,l}\}$ are only rotationally invariant. To obtain RS invariants, these invariants must be subjected to a normalization. Using $I_{2,0}$ as a criterion, we can get RS invariants based on the property (5):

$$P_{4,0} = \frac{I_{4,0}}{(I_{2,0})^2}, P_{6,0} = \frac{I_{6,0}}{(I_{2,0})^3}, P_{8,0} = \frac{I_{8,0}}{(I_{2,0})^4}, \quad (17)$$

which are independent of the angular distribution of the SDF:

$$\begin{aligned} P_{2,1} &= \frac{I_{2,1}}{(I_{2,0})^2}, P_{4,1} = \frac{I_{4,1}}{(I_{2,0})^4}, \\ P_{4,2} &= \frac{I_{4,2}}{(I_{2,0})^4}, P_{4,3} = \frac{I_{4,3}}{(I_{2,0})^3}, \\ P_{4,4} &= \frac{I_{4,4}}{(I_{2,0})^4}, \end{aligned} \quad (18)$$

which include the information of the angular distribution of the SDF.

3 Experiments

Sixteen natural textured images from the Brodatz album are used (see Table 1). The image sizes are 128×128 and 64×64 , and the integral radius $R(\alpha)$ is determined by setting $\gamma = 0.9$ in (4). The process of the classification experiment is as follows. Each of the 16 textured images are rotated by every 15 degrees($0^\circ \sim 75^\circ$) and magnified by $2^{n/3}$ ($n = 0, \pm 1, \pm 2, \pm 3$) times using bilinear interpolation. A total of $16 \times 6 \times 7$ images are obtained. Moment invariants are estimated for every image.

Then a leave-one-out strategy is adopted, i.e., after one image(as a test image) is left out, means and covariance matrices of invariants for the remaining images are computed. Finally, the test image is classified based on the Mahalanobis distance. This process is repeated for all the images. The average classification accuracy rates are listed in Table 2. The fact that the results of (3) in Table 2 is superior to that of (4) means that the radial distribution of the SDF of the images used here has more information than the angular distribution. The result with image size 64×64 is a little inferior to that with 128×128 ; this means that the 64×64 image is too small to be regarded as statistically homogeneous.

Another experiment was carried out, where test images of the 16 kinds were newly taken from the Brodatz album in order to avoid the low-pass filtering effect brought by the bilinear interpolation. The test image size is 128×128 with the scaling factor $\alpha = 1.35$ and the training images are the synthesized ones. All the test images are correctly recognized using all the invariants in (17) and (18).

Table 1 Textures used in experiments

#1	D24: leather	#9	D11: woolen cloth
#2	D93: fur	#10	D17: weave
#3	D4 : cork	#11	D82: straw cloth
#4	D5 : mica	#12	D84: raffia
#5	D9 : grass	#13	D95: brick wall
#6	D12: tree bark	#14	D37: water
#7	D73: bubbles	#15	D68: wood grain
#8	D92: pigskin	#16	D15: straw

Table 2 Classification results.

	Invariant Parameters	Accuracy Rate	
		128×128	64×64
(1)	$P_{2,1}, P_{4,0}$	94.5%	79.9%
(2)	$P_{2,1}, P_{4,0}, P_{6,0}$	98.7%	94.6%
(3)	$P_{2,1}, P_{4,0}, P_{6,0}, P_{8,0}$	99.9%	94.8%
(4)	$P_{2,1}, P_{4,0}, P_{4,1}, P_{4,2}, P_{4,3}, P_{4,4}$	99.1%	93.8%
(5)	$P_{2,1}, P_{4,0}, P_{4,1}, P_{4,2}, P_{4,3}, P_{4,4}, P_{6,0}, P_{8,0}$	100%	97.2%

4 Stability Analysis

Finally we discuss the robustness of the invariants $P_{n,l}$'s against the change of scale. We assumed that the SDF decreases rapidly as frequency increases and the property of the moments represented by (5) holds. As a matter of fact, the SDF often does not decrease so rapidly and an imaging system usually provides a low-pass filter to avoid aliasing. These effects make the property (5) approximately correct. However, the deviation errors of the moments appeared in the numerator and the denominator of $P_{n,l}$'s in (17) and (18), when scaled, have the same sign and nearly the same relative magnitudes. Therefore, they cancel each other, which makes $P_{n,l}$'s sufficiently good invariants to scaling.

In the following, we confirm it theoretically by assuming a simple form of the SDF and experimentally by using real images photographed with different focal lengths.

First, we theoretically analyse the stability of the moments and invariants based on the SDF of the following simple form

$$\begin{aligned} S(\omega, \nu) &= S(\rho) = \frac{\sigma^2}{(\rho^2 + a^2)^2}, \\ \rho &= \sqrt{\omega^2 + \nu^2} \end{aligned} \quad (19)$$

where a is a parameter representing the width of the SDF and the scaling factor α is inversely proportional to a . We assume $S(\rho)$ outside the circle with the radius π is put to zero, which represents the effect of the low-pass filter for preventing aliasing. The total power inside a circle with the radius R is given by

$$2\pi \int_0^R S(\rho) \rho d\rho = \pi \sigma^2 \left(\frac{1}{a^2} - \frac{1}{R^2 + a^2} \right). \quad (20)$$

Applying this relation to (4), we decide R as follows

$$R = \frac{\sqrt{\gamma}\pi a}{\sqrt{a^2 + (1-\gamma)\pi^2}}. \quad (21)$$

Here we obtain the two rotation invariants $I_{2,0}$ and $I_{4,0}$ using the SDF (19),

$$I_{2,0} = \frac{\sigma^2}{2} \left[\ln \frac{R^2 + a^2}{a^2} + \frac{a^2}{R^2 + a^2} - 1 \right], \quad (22)$$

$$I_{4,0} = \frac{\sigma^2}{2} \left[R^2 - 2a^2 \ln \frac{R^2 + a^2}{a^2} - \frac{a^4}{R^2 + a^2} + a^2 \right]. \quad (23)$$

We also examine the RS invariant $P_{4,0}$

$$P_{4,0} = \frac{2}{\sigma^2} \frac{R^2 + a^2 - 2a^2 \ln \frac{R^2 + a^2}{a^2} - \frac{a^4}{R^2 + a^2}}{\left[\ln \frac{R^2 + a^2}{a^2} - \frac{R^2}{R^2 + a^2} \right]^2}. \quad (24)$$

Since the variance of the grey level is normalized, the total power of the SDF inside the circle with the radius π is constant and we put it 1, which leads to

$$\pi \sigma^2 \left(\frac{1}{a^2} - \frac{1}{\pi^2 + a^2} \right) = 1. \quad (25)$$

This gives σ^2 as a function of a .

Figure 1 shows the relative changes of three quantities, $\alpha^2 I_{2,0}$, $\alpha^4 I_{4,0}$, and $P_{4,0}$ when the scale factor α varies from 1 to 0.25, corresponding to the range of a from $\pi/16$ to $\pi/4$. These three must be constant if the property (5) exactly holds. The quantities, $\alpha^2 I_{2,0}$ and $\alpha^4 I_{4,0}$, are not constant in Fig.1 and therefore the deviations of $I_{2,0}$ and $I_{4,0}$ from the relation (5) are fairly large. On the contrary, $P_{4,0}$ in Fig.1 is nearly constant, for example, the relative deviation is only 12.5% for scale change up to 4. The reason is that since the deviations of $(\alpha^2 I_{2,0})^2$

and $\alpha^4 I_{4,0}$ have the same signs and nearly the same magnitudes, $P_{4,0}$ defined as the ratio of these two quantities is nearly constant.

Second, we examine the stability of the invariants using the two textured images from Brodatz album at different scales. The two images are *cork* and *bark of tree*; the SDF of the former is isotropic and decreases comparatively rapidly while that of the latter is anisotropic and decreases slowly in a certain direction. The results of three invariants same as appeared in Fig.1 are shown in Fig.2 for cork and Fig.3 for bark of tree. The image used as $\alpha = 1$ is a scanner-input one and other three images are CCD-camera ones with different focal lengths. The deviations shown in Fig.2 and Fig.3 are larger than those in Fig.1 but the relative deviations of $P_{4,0}$'s are within 15% at scale change up to 2. Although the form of the real image SDF is complicated, the stability of $P_{4,0}$ is consistent with the theoretical analysis using the model SDF. Therefore, the scale invariants, not only $P_{4,0}$ but also other $P_{n,l}$'s, are robust enough to scale change because other $P_{n,l}$'s are defined as the same structure as $P_{4,0}$ in (17) and (18).

5 Conclusion

We proposed the method for classifying rotated and scaled textured images using rotation and scale invariants based on spectral moments. The experimental results confirmed the effectiveness of the method. The robustness of the invariants was explained theoretically and confirmed experimentally.

References

- [1] F.S.Cohen, Z.Fan and M.A.Patel, "Classification of Rotated and Scaled Textured Images Using Gaussian Markov Random Field Models", IEEE Trans. Patt. Anal. Machine Intell., PAMI-13, 2, pp.192-202, Feb. 1991.
- [2] Y.Wu and Y.Yoshida, "An Efficient Method for Rotation and Scaling Invariant Texture Classification", Proc. IEEE ICASSP, (Detroit) pp.2519-2522, May 1995.
- [3] S.A.Dudani et al. , "Aircraft Identification by Moment Invariants", IEEE Trans. Computer, C-26, pp.39-45, Jan. 1977.
- [4] M.R.Teague,"Image Analysis via the General Theory of Moments", J. Opt. Soc. Am., Vol.70, No.8, pp.920-930, Aug. 1980.
- [5] C. Teh and R. T. Chin, "On Image Analysis by the Methods of Moments", IEEE Trans. Patt. Anal. Machine Intell., PAMI-10, 4, pp.496-513, July 1988.

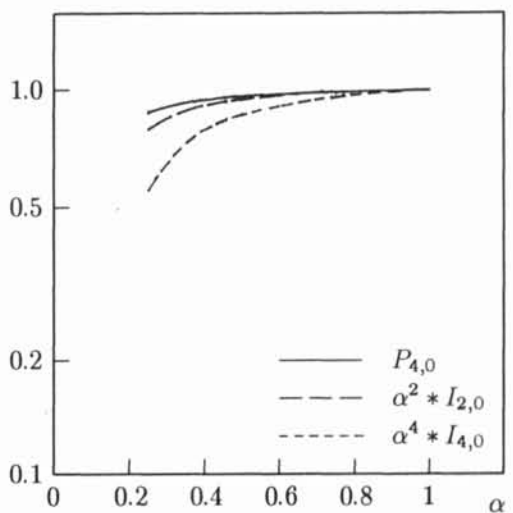


Figure 1: Relative changes of invariants vs α for the SDF (19)

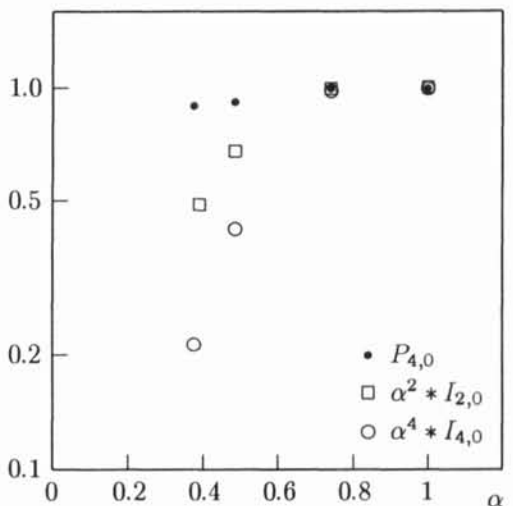


Figure 2: Relative changes of invariants vs α for cork

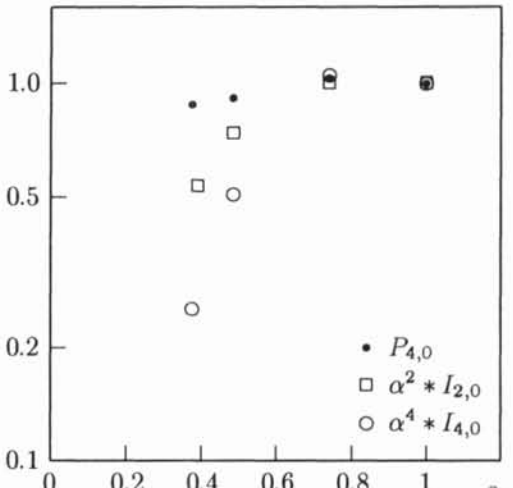


Figure 3: Relative changes of invariants vs α for bark of tree